Published in final edited form as:

Mol Pharm. 2014 February 3; 11(2): 531–544. doi:10.1021/mp4005029.

Formulation and Characterization of Nanoemulsion Intranasal Adjuvants: Effects of Surfactant Composition on Mucoadhesion and Immunogenicity

Pamela T. Wong[1], **Su He Wang**[1], **Susan Ciotti**[2], **Paul E. Makidon**[1], **Douglas M. Smith**[1], **Yongyi Fan**[1], **Charles F. Schuler IV**[1], and **James R. Baker Jr.**[1,2,*]

[1]Michigan Nanotechnology Institute for Medicine and Biological Sciences and Department of Internal Medicine, University of Michigan Medical School, Ann Arbor, Michigan

[2]NanoBio Corporation, Ann Arbor, Michigan

Abstract

Development of effective intranasal vaccines is of great interest due to their potential to induce both mucosal and systemic immunity. Here we produced oil-in-water nanoemulsion (NE) formulations containing various cationic and nonionic surfactants for use as adjuvants for the intranasal delivery of vaccine antigens. NE induced immunogenicity and antigen delivery are believed to be facilitated through initial contact interactions between the NE droplet and mucosal surfaces which promote prolonged residence of the vaccine at the site of application, and thus cellular uptake. However, the details of this mechanism have yet to be fully characterized experimentally. We have studied the physicochemical properties of the NE droplet surfactant components and demonstrate that properties such as charge and polar head group geometry influence the association of the adjuvant with the mucus protein, mucin. Association of NE droplets with mucin *in vitro* was characterized by various biophysical and imaging methods including dynamic light scattering (DLS), zeta potential (ZP), and surface plasmon resonance (SPR) measurements as well as transmission electron microscopy (TEM). Emulsion surfactant compositions were varied in a systematic manner to evaluate the effects of hydrophobicity and polar group charge/size on the NE-mucin interaction. Several cationic NE formulations were found to facilitate cellular uptake of the model antigen, ovalbumin (OVA), in a nasal epithelial cell line. Furthermore, fluorescent images of tissue sections from mice intranasally immunized with the same NEs containing green fluorescent protein (GFP) antigen demonstrated that these NEs also enhanced mucosal layer penetration and cellular uptake of antigen *in vivo*. NE-mucin interactions observed through biophysical measurements corresponded with the ability of the NE to enhance cellular uptake. Formulations that enhanced antigen uptake *in vitro* and *in vivo* also led to the induction of a more consistent antigen specific immune response in mice immunized with NEs containing OVA, linking NE-facilitated mucosal layer penetration and cellular uptake to enhancement of the immune response. These findings suggest that biophysical measurement of the

[*]To whom correspondence should be addressed Tel.: 734-647-2777; fax: 734-936-2990; (jbakerjr@umich.edu).

SUPPORTING INFORMATION: Supplemental methods and figures are provided as described in the text. This material is available free of charge via the Internet at http://pubs.acs.org.

mucoadhesive properties of emulsion based vaccines constitutes an effective *in vitro* strategy for selecting NE candidates for further evaluation *in vivo* as mucosal adjuvants.

Keywords

Adjuvant; Intranasal Vaccine; Nanoemulsion; Mucoadhesion; Oil-in-water emulsion

INTRODUCTION

Mucosal vaccination offers unique advantages over parenteral vaccination in the prevention of infectious diseases such as the induction of both mucosal and systemic immunity compared to solely systemic immunity for subcutaneous and intramuscular vaccines. [1-5] Administration of a vaccine to a mucosal surface can induce immunity at multiple mucosal sites in addition to the application site. [3, 5, 6] Nasal immunization, for example, can induce antigen-specific antibody production and a cellular memory response in the respiratory tract as well as in the genital tract mucosa. [5-7] The nasal cavity is a prime site for vaccination as it is easily accessible, has a moderately permeable epithelium with a high availability of immune-reactive sites, and provides minimal exposure to degradative environments. [3, 8] Intranasal (IN) vaccines are currently in development for the prophylaxis of pathogens such as *Neisseria meningitidis*, respiratory syncytial and herpes simplex type 2 viruses, and are licensed for influenza virus. [7, 9-14] As infectious diseases transmitted through mucosal surfaces may be most effectively prevented through mucosal immunity, development of compounds that are both effective adjuvants and delivery agents for IN antigen administration is highly desirable.

Several adjuvants enhance immune response induction by providing a sustained release of antigen at a specific site through a depot effect. [15, 16] For IN vaccines, the mucous layer presents both a barrier to antigen and adjuvant uptake by the epithelia and dendritic cells (DCs) as well as a site for vaccine deposition. Here we developed bioadhesive nanoemulsion adjuvants for IN administration with the hypothesis that greater mucoadhesion leads to longer retention in the nasal mucosa, facilitating antigen-adjuvant permeation across the mucous layer and cellular uptake (Figure 1). Oil-in-water nanoemulsions (NEs) are nanoscale (200–700 nm in diameter) droplets composed of a combination of surfactants, a co-solvent (ethanol), oil (soybean oil), and water. [17] We have shown that as an adjuvant for hepatitis B surface antigen (HBsAg), NEs induce systemic immunity comparable to injected aluminum-based hepatitis vaccines. [17] Furthermore, they produced mucosal and cellular immune responses not elicited by conventional injectable vaccines, uniquely activated cytokine production by the nasal ciliated epithelium and promoted DC trafficking. [18] Effective NE adjuvanticity for whole influenza and vaccinia viruses, recombinant anthrax protective antigen, and HIV gp120 have also been demonstrated. [19-22]

The mucus layer on the surface of nasal epithelial cells plays a critical role in host defense mechanisms through adhesion and entrapment of invading virus particles and bacteria. [23] The efficiency of NE-facilitated antigen delivery in the nasal epithelium likely relies upon similar mucoadhesive interactions. To evaluate the mucoadhesive properties of NEs, association with mucin, which constitutes the major protein component of mucus was studied.[24, 25] Mucins are a family of heavily glycosylated proteins that form large aggregates (MW = 0.5-40 MDa) and carry a large amount of negative charge, primarily due to the sialic acid (*N*-acetylneuramic acid), sulfate, and carboxylate groups present on these glycoproteins. While some mucins are membrane anchored, most are secreted and form a layer adherent to epithelial cells.[24] Association with mucin has been used previously to evaluate mucoadhesive properties of polymers such as chitosan and synthetic cationic copolymers *in vitro*.[26-29]

Here we produced a number of NE formulations each prepared by varying the combinations of nonionic and ionic surfactants which were chosen based on their hydrophilic-lipophilic balance (HLB) values and polar head groups. We performed a series of biophysical studies, *in vitro* cell-based assays, and *in vivo* IN immunization studies in order to determine the mechanistic aspects of the NE-mucin interaction, specifically by assessing how surfactant compositions influenced NE-mucin association in solution and on biosurfaces and how they impacted the structure of the droplet upon binding. We found that the mucoadhesive properties of NEs measured *in vitro* were directly related to their ability to induce immunogenicity *in vivo*. We believe that these biophysical studies provide data that could be used as one of the early screening parameters to predict vaccine efficacy. This strategy is potentially valuable for large scale evaluation of mucosal vaccines or drug delivery systems and would allow for rapid screening of candidate formulations.

METHODS

Preparation of Nanoemulsions

NE formulations were provided by NanoBio Corporation, Ann Arbor, MI. Briefly, NEs were manufactured by high-speed emulsification of ionic and nonionic surfactants, ethanol (200 proof), soybean oil and purified water using a high speed homogenizer. Nonionic surfactants including sorbitan (Span), polysorbate (Tween), and poloxamer surfactants, and ionic surfactants and their abbreviations are listed in Table 1. Emulsions are annotated according to blend ratios of ionic to nonionic surfactants. A CPC/Tween80 NE annotated as 1:6 contains one part CPC to six parts Tween80 (by weight), and a Tween80 NE with no cationic surfactant is annotated as 0:6. For vaccine formulations and antigen incorporation experiments, NE stocks at 60% (w/w) were mixed with 10 mg/mL hen egg white ovalbumin fraction V (OVA) (Sigma-Aldrich) in 10× phosphate-buffered saline (PBS), pH 7.4 and sterile water for injection for 10 min to achieve a final concentration of 20% NE (w/v) with the specified amount of OVA for each application in PBS, pH 7.4.

Dynamic Light Scattering (DLS) and Zeta Potential (ZP)

DLS and ZP measurements were performed consecutively for the same sample on a Zetasizer Nano–ZS (Malvern Instruments Ltd). Porcine gastric mucin type III (mixture of different mucins) (Sigma-Aldrich), was rehydrated at 1 mg/mL in 1 mM HEPES pH 7 at room temperature (RT) for 30 min. 0.1% NE (w/v) was mixed with 0.05 mg/mL mucin in 1 mM HEPES pH 7, at RT for 2 min before measurement. Particle sizes (PS) are expressed as average diameter (Z_{ave}d). For DLS and ZP measurements of NE droplets with incorporated antigen, Tween80 0:6, CPC/Tween80 1:6, or CPC/P407 1:6 NEs a final concentration of 20% (w/v) NE with 1 mg/mL OVA in PBS. To obtain the PS for these formulations, the mixture was diluted to a final concentration of 0.1% (w/v) NE containing 0 or 5 μg/mL OVA in PBS, pH 7.4. For ZP measurements, the mixture was diluted to the same concentrations in 1 mM HEPES pH 7 and incubated with or without 0.05 mg/mL mucin. For ΔZ_{ave} measurements with mucin, 0.1% (w/v) NE-OVA (formed in PBS) was mixed with 0.05 mg/mL mucin in 1 mM HEPES pH 7. Reported error for size measurements was calculated as standard deviation from measured polydispersity index (PdI) values. Error for ZP measurements is reported as actual measurement zeta deviation values.

Surface Plasmon Resonance (SPR)

SPR binding experiments were performed on a Biacore® X instrument (GE Healthcare). Immobilization of mucin to a CM4 sensor chip (flow cell 1) was performed following an aldehyde-carbohydrazide coupling protocol in which the oxidized mucin was reductively immobilized to the biochip surface following the manufacturer's protocol. Oxidized mucin at 0.5 mg/mL in acetate buffer, pH 4 was injected twice over the ligand channel (flow cell 1), followed by reductive treatment with sodium cyanoborohydride, resulting in an increase in response units (RU) of 6,300, equivalent to a mucin immobilization density of 6.3 ng/mm^2. The reference channel (flow cell 2) on the same chip was treated in the same way but without injection of oxidized mucin. In these studies flow cell 2 serves as an additional positive control surface rather than a true inert reference channel because it presents a layer of negatively charged carboxylate groups which is very similar to the mucin glycosyl groups. 0.0125% NE (w/v) (unless otherwise specified) in 1 mM HEPES pH 7.0 was injected over the ligand and reference channels at a flow rate of 1 μL/min. At the end of each dissociation phase, NEs dissociated completely from the chip. SPR sensorgrams were fitted to extract kinetic parameters such as the rate of dissociation (k_{off}). [30]

Transmission Electron Microscopy (TEM)

NE and mucin samples for TEM were prepared similarly as for zetasizing. 0.1% (w/v) NE was mixed with or without 0.05 mg/mL mucin in 1 mM HEPES pH 7.0 for 10 min. 5 μL of the samples were placed on 200 mesh carbon coated copper grids for 10 min, air-dried, rinsed with dH_2O, and stained with 1.0% uranyl acetate for 10 min. Excess stain was removed, and the grids were air-dried. Images were collected with a Philips CM-100 transmission electron microscope at 100 kV.

Epithelial Cell Uptake

To evaluate NE facilitated uptake of OVA in epithelial cells and adhesion of NE to cell surface localized mucin, RPMI 2650 human nasal cells (ATCC) were seeded overnight on chambered coverglasses in Eagle's media (with 10% heat-inactivated FBS). NE and Alexafluor 488 conjugated OVA (A488-OVA) were mixed and added to cells to a final concentration of 0.1% CPC/Tween 80 1:6 (w/v) with 20 μg/mL A488-OVA for 1.5 h in media at 4 °C or 37 °C. Cells were washed with PBS, fixed for 20 min in 4% paraformaldehyde, and preserved in Prolong Gold with DAPI (Life Technologies). Cells were imaged on a Leica inverted SP5X confocal microscope (Leica Microsystems).

Animals

Eight-week-old female outbred CD-1 mice (Jackson Laboratories) for histological imaging, and 8-week-old female C57BL/6 mice (Charles River Laboratories) for immunogenicity studies were housed in specific pathogen-free conditions. All procedures were approved by the University Committee on the Use and Care of Animals (UCUCA) at the University of Michigan.

Tissue Identification and Antigen Localization

Mice were immunized IN with 10 μL/nare of 10 μg enhanced green fluorescent protein (GFP) (total/mouse) (BioVision Research Products) alone or with 20% NE (w/v), and sacrificed 16-18 hr post-inoculation. The nasal epithelium was isolated and frozen in Tissue-Tek OCT (Sakura Finetek) with liquid nitrogen, and slides containing 5 mm tissue sections were prepared. GFP distribution was imaged with a Leica DCS 480 epifluorescence microscope and analyzed with LAS software (Leica Microsystems). For light microscopy with the reference nasal epithelium, the nasal epithelium from a mouse immunized with PBS only was isolated, embedded in paraffin, and sectioned. Tissue samples were stained with Light Green Counterstain (Genetex) and TUNEL, and viewed on a conventional light microscope.

Immunogenicity

C57BL/6 mice were immunized IN with two administrations, 4 weeks apart, of 15 μL (7.5 μL/nare) of a NE (20% w/v) and OVA (20 μg/mouse) mixture (NE-OVA) prepared as described above, or of OVA alone in PBS, pH 7.4. This antigen dosage was determined to be optimal in our previous studies (unpublished results). OVA used for vaccination was endograde OVA (Hyglos GmbH). NE formulations evaluated were of the CPC/Tween80 series (0:6, 1:40, 1:20, 1:6). Treatment groups consisted of either 5 (OVA alone, OVA with 0:6 or 1:6) or 10 mice (OVA with 1:20 or 1:40). A separate group of mice was immunized with 20% CPC/Tween80 1:6 (n=5) or CAB/Tween80 1:6 (n=5) with the same amount of OVA.

Serum was obtained from the saphenous vein every 2-weeks post-initial immunization, and anti-OVA specific IgG was measured by ELISA using microtiter plates coated with 20 μg/mL OVA. For average IgG, serum from each mouse was diluted 1:200 in PBS with 0.1% BSA. For end-titers, serum samples from individual mice were serially diluted in PBS with 0.1% BSA. Samples were incubated on the coated plates for 1 hr at 37°C. After washing the plate with PBST, the plate was incubated with goat anti-mouse IgG-alkaline phosphatase for an additional hour at 37 °C. After final washing, the plate was developed with Sigma FastTM (Sigma-Aldrich) AP substrate according to the manufacturer's protocol, and the optical density (OD) was measured at 405 nm (OD_{405nm}). Endpoint titers are reported as the reciprocal of the highest serum dilution producing an optical density (OD) above a cutoff value (sum of the OD of the same dilution of a control serum from an untreated mouse and two standard deviations).

Statistical analysis

Microsoft Excel 2010 and Graph Pad Prism 6 were used for graphing and statistical analyses. Comparisons were be made between groups using ANOVA when continuous outcome variables were normally distributed and Kruskal-Wallis when not normally distributed; Dunn's adjustment for multiple comparisons was used.

RESULTS

Dynamic Light Scattering and Zeta Potential Measurements

NE association with mucin was evaluated by determining the particle size distribution using dynamic light scattering (DLS) and by measuring NE surface charge (zeta potential (ZP)) before and after mucin addition. Figure 2A shows an example of a number weighted particle size distribution for mucin alone, the CPC/Tween80 1:6 NE alone, and the co-incubated mixture. While free mucin alone has the potential to form large aggregates, it is highly polydisperse, and its size distribution did not overlap significantly with that of NE alone at these concentrations. The size distribution of the mixture of mucin with CPC/Tween80 1:6 showed a factor of >4 increase in the mean diameter value (Z_{ave}), indicative of adhesive interactions between mucin and the NE. We extended the measurements to other NE formulations, each containing mixtures of nonionic surfactants (Span, Tween, Poloxamer) with cationic (CPC, DODAC, BCl, BZT, CTAC, StrCl), zwitterionic (CAB) or anionic (SDS) surfactants (abbreviations listed in Table 1). These NEs had mean diameters ranging from 200-900nm. Emulsions are annotated according to blend ratios (wt/wt) of ionic to nonionic surfactants (ex. CPC/Tween80 1:6 contains one part CPC to six parts Tween80, Tween80 0:6 contains no cationic surfactant). All formulations had unimodal size distributions with low polydispersity (PdI$\leq$ 0.2) (Figure 2B). The surface charge (ZP) of each NE was dictated by the charge of the ionic surfactant component. NEs with increasing ratios of cationic to nonionic surfactants such as 0:6, 1:40, 1:20 and 1:6, CPC/Tween80 exhibited an incremental increase in ZP, reflecting increasing positive surface charge (Figure 2C). Increasing the CPC for Tween80 NEs from 0:6 to 6:1 for instance, increased the ZP by 78 mV.

Incubation of NE with mucin increased the particle size (ΔZ_{ave}=$Z_{ave\ final}$−$Z_{ave\ init}$) and decreased the surface charge ($\Delta ZP = ZP_{init} - ZP_{final}$) of most NEs containing cationic surfactants (initial refers to the value pre-mucin addition, and final refers to post-mucin addition). In particular, CPC/Tween80 1:6, the adjuvant used in the *in vivo* studies below and in previous adjuvanticity studies [17] showed a very large increase in particle size (ΔZ_{ave}) of 1546.0 nm upon addition of mucin, supporting the association of this NE with mucin and the formation of a large complex in solution. Furthermore, mucin reduced the ZP of this NE from 59.9±6.1 to 0.5±3.4 mV (ΔZP of 59.4 mV) (Figure 2 C and Figure S2). Mucin has a substantial negative charge, and as it coats the NE, positive surface charge from the cationic surfactant is neutralized (Figure 2C). The formulations studied included CPC and non-CPC containing NEs combined with various nonionic surfactants. Figure 2 shows the changes in particle size and charge upon mucin addition for select NEs, and Figure 3 summarizes the effect of mucin addition for the entire set of NE formulations in scatter plots of ΔZP and ZP_{init}, plotted versus ΔZ_{ave}.

The ΔZ_{ave} and ΔZP of the NEs highlighted in Figures 2B & C demonstrated that formulations exhibited diverse mucin associative properties as modulated by their surfactant composition. In the subset of NEs shown in Figure 2, three different types of NE-mucin interactions were observed: those with large ΔZP and large ΔZ_{ave}, those with large ΔZP but small or no ΔZ_{ave}, and those with small or no ΔZP and ΔZ_{ave}. These patterns were strengthened upon expanding the screening to our entire set of compounds for their interaction with mucin (Figure 3), and we found that all formulations could be clustered into these three general groups or families based on their association with mucin, which would be expected to translate into differences in *in vivo* activity.

Evaluation of the entire set of NE formulations revealed several important trends. A positive ZP_{init} was required for NE-mucin association (Figure 3B & D). Tween80 0:6, which had no cationic surfactant, had a similar initial $Z_{ave\ init}$ (417.9 nm) as CPC/Tween80 1:6, but had a slightly negative ZP_{init}, and gave ΔZ_{ave} and ΔZP values near zero upon mucin addition (Figures 2B & C and Figure S2). Furthermore, zwitterionic CAB/Tween80 1:6 ($Z_{ave\ init}$ = 529.2 nm), and anionic SDS/Tween80 1:6 ($Z_{ave\ init}$ = 700 nm) (Figure S1) both gave only low ΔZ_{ave} values of 18.1 nm and 21.8 nm, and minimal ΔZP values of 4.7 mV and −5.9 mV, respectively (Figure 2B & C and Figure S2). Since these NEs share the same nonionic components (Tween80, soybean oil), mucin association is largely attributable to the cationic surfactant.

Scatter plots revealed that charge is not the only factor dictating the magnitude of ΔZ_{ave} or ΔZP, as several NEs with the same surface charge (ZP_{init}) had dramatically different ΔZ_{ave} values (Figure 3B & D and Figure S2). Furthermore, a large ΔZP value did not always correspond to a large ΔZ_{ave} value, as some NEs with a large ΔZP (>20 mV) had ΔZ_{ave} values <100 nm (Figure 3A & C and Figure S2). This is illustrated by the DODAC/Tween80 1:6 NE which has both $Z_{ave\ init}$ and ZP_{init} values (538.5 nm, 50.5±4.8 mV) similar to CPC/Tween80 1:6 (406.7nm, 59.9±6.1 mV). However, incubation of DODAC/Tween80 with mucin resulted in only a small ΔZ_{ave} value of 41.1 nm, but gave a large ΔZP of 68.6 mV, comparable to that of CPC/Tween80 1:6 (59.4 mV) (Figure 2C and Figure S2). CPC (HLB=26) is a single chain cationic surfactant, and is more hydrophilic than DODAC (HLB ~10) as its dual acyl chain prefers the oil:water interface (Figure S1). Thus the polar group of CPC likely protrudes further from the droplet surface than DODAC, allowing it to interact differently with mucin.

The structure and physicochemical properties of the nonionic surfactants also affected the mucin interaction. For example, while CPC/P407 1:6 contains an equivalent amount of CPC as CPC/Tween80 1:6, it has a much reduced surface charge (ZP_{init} = 29.9±5.7 mV) (Figure 2C). We believe that this is due to the differences in the hydrophilicity and the structures of the nonionic surfactants. P407 (HLB = 22) is more hydrophilic than Tween80 (HLB = 15), and thus the two bulky extended hydrophilic polyethylene glycol groups of P407 protruding from the oil:water interface may more effectively shield the positive charge of CPC on the surface (Figure S1). CPC/P407 1:6, had a ΔZ_{ave} of only 15.5 nm, and a ΔZP of 21.5 mV, which resulted in neutralization of the droplet (Figure 2B & C and Figure S2). Increasing the CPC content in CPC/P407 to a 6:1 ratio (ZP_{init}=60.3±7.5 mV), still gave a much smaller ΔZ_{ave} (262.6 nm) relative to CPC/Tween80 1:6. Additionally, the ΔZP magnitude varied significantly for different cationic NEs, reflecting variable degrees of NE droplet coating depending on both cationic and nonionic surfactants**.** Thus, while positive surface charge is necessary for association, other factors also influence the interaction. However, all neutral or negatively charged NEs consistently gave no significant changes in Z_{ave} or ZP with mucin.

Finally, we note that the ratio of ionic to nonionic surfactant leads to a nonlinear variation in the mucin associative properties. Within a series of NEs sharing the same nonionic surfactant, a stepwise correlation between CPC content and ΔZ_{ave} and ΔZP with mucin was observed. Increasing the CPC ratio in the CPC/Tween80 series NEs from 0:6 to 1:40 and 1:20 increased the ZP_{init} to 12.4±6.3 mV and 30.9±4.8 mV, respectively, while ΔZ_{ave} upon mucin addition for both remained <35nm (Figure 2B). At 1:6, 1:1 and 6:1, very large ΔZ_{ave} values of 1546 nm, 721.9 nm and 496.5 nm, were observed respectively, suggesting that above a threshold level of CPC (1:6), multiple NE droplets can associate by binding to the same mucin molecules (Figure 2B and Figure S2). A steady increase in the ΔZP magnitude was also observed as CPC was increased. Interestingly, increasing the CPC above 1:6 did not significantly alter the magnitude of ΔZP, possibly reflecting saturation of the droplet with the maximal number of mucin molecules that can be sterically accommodated on the surface of a 400 nm droplet. These DLS and ZP studies suggest that many of the NEs share physicochemical properties, yet have strikingly different ΔZP and ΔZ_{ave} values with mucin depending on the surfactant composition. To further confirm that changes in ZP and Z_{ave} corresponded to association with mucin, the amount of mucin adsorbed on the NE droplet was determined for representative NEs by separating free mucin from bound mucin (Figure S5). We found that a drop in ZP and increase in Z_{ave} upon incubation with mucin did indeed correspond with an increase in droplet associated mucin. We suggest that such characterization of NE-mucin interactions in solution provides biophysical parameters important for selecting optimal compositions of NE adjuvants for further evaluation as IN vaccines. To determine whether antigen incorporation on the NE alters the droplet properties, the DLS and ZP measurements were repeated for NE premixed with ovalbumin antigen (OVA) under conditions similar to the vaccination mixture used *in vivo* as described in the supplementary information. OVA incorporation slightly lowered the ZP_{init} of CPC containing NEs, but the general trends observed for the ΔZ_{ave} and ΔZP values for the same NE formulations without antigen were retained (Table S1), demonstrating that biophysical properties characteristic of each NE applies to the NE with antigen as well. We selected the CPC/Tween80 and CPC/P407 series, and DODAC/Tween80, CAB/Tween80 and SDS/Tween80 formulations as representative NEs for further characterization, as they share several physicochemical properties, yet have strikingly different ΔZP and ΔZ_{ave} values with mucin.

Dissociation Kinetics (Surface Plasmon Resonance Spectroscopy)

DLS and ZP methods measure the association of NE and mucin in solution under equilibrium conditions. While this solution-based method provides insight on the binding to secreted mucins, we were also interested in studying adhesion kinetics to mucins anchored to the epithelial layer surface. SPR spectroscopy was employed to measure association and dissociation kinetics on a surface on a real-time basis.

Mucin was immobilized on a CM4 sensor chip surface as a model for the epithelial surface as described in the methods section. Binding kinetics for representative NEs (CPC/Tween80 series (0:6, 1:6, 1:1, 6:1)) to the model surface are shown in Figure 4. CPC/Tween80 1:6 showed significant adhesion to the mucin-immobilized surface (Mucin/CMC) (Figure 4A) as well as some adhesion to the reference cell which consisted of the unconjugated carboxymethylated surface (CMC) (Figure 4B). Adhesion of all four NEs was higher to the mucin surface than to the CMC reference surface—demonstrating that a significant portion of the observed binding was mucin-specific (Figure 4C). Binding to both channels occurred in a dose dependent manner, and was eliminated upon increasing the ionic strength of the solution (Figure S4). Binding to the reference channel was not surprising, as the unmodified CMC surface is negatively charged, and the negative carboxylate groups of the carboxymethylated cellulose resemble the negatively charged sialic acid groups of mucin. These results confirm the DLS and ZP results which suggested that NE adhesion to mucin is driven by electrostatic attraction.

Tween80 0:6 exhibited minimal binding followed by rapid dissociation. Increasing the CPC content in CPC/Tween80 led to an enhancement in the amount of association (greater RU) on both the mucin and the CMC surfaces. Since mucin likely associates with the CPC and the nonionic surfactants and oil as well, classical ligand binding models were not applicable, complicating quantitative kinetic analysis. We chose to fit the binding curves to determine dissociation rates (k_{off}) as this value is independent of ligand concentration. Inclusion of CPC reduced the NE dissociation rate by nearly two orders of magnitude relative to that of Tween80 0:6, reflecting a greater mucin affinity for NEs containing CPC. k_{off} for Tween80 0:6 as calculated from the subtracted sensorgram was 8.7 (± 4.6) × 10^{-1} s^{-1} as compared to 8.1 (± 0.2) × 10^{-3} s^{-1} for CPC/Tween80 1:6. k_{off} values for CPC/Tween80 1:1 and 6:1 were along the same order of magnitude as 1:6 (1.6 × 10^{-2} s^{-1} and 1.7 × 10^{-2} s^{-1}, respectively). However the curve fits gave high error values, likely due to greater background binding attributable to increased association with the CMC surface itself as well.

While mucin association is important for antigen delivery, exceedingly slow dissociation of the adjuvant will lead to removal through mucociliary clearance. Even with a CPC ratio of 6:1, the interaction of CPC/Tween80 with mucin displays a relatively fast dissociation as compared to typical multivalent receptor-ligand interactions, perhaps enabling NEs to bind to, yet diffuse through the mucous layer effectively.

Transmission Electron Microscopy (TEM)

In the above DLS and ZP measurements, certain NEs had changes in Z_{ave} with mucin much larger than expected for association of a single mucin layer, yet exhibited ΔZP values of the same magnitude as those with much smaller ΔZ_{ave} values. TEM analysis was performed in order to further investigate the morphologies of these different NE-mucin complexes. CPC/Tween80 1:6 and DODAC/Tween80 1:6 were examined because of their similar ZP_{init} and particle size, as well as ΔZP, but strikingly different ΔZ_{ave} values. Tween80 0:6 was also examined. NE was incubated with mucin under the same conditions used in the DLS and ZP measurements.

TEM revealed dramatic differences between the structures of CPC/Tween80 and DODAC/Tween80 upon binding mucin (Figure 5). Alone, mucin appeared as a diffuse homogenous field of protein (Figure 5A), and CPC/Tween80 (Figure 5B) and DODAC/Tween80 (not shown) as spherical droplets of relatively uniform size. In the presence of mucin, CPC/Tween80 bound and sequestered most of the mucin, and the NE droplets coalesced into larger droplets 700-1500 nm in diameter, with many reaching >10 μm (Figure 5C). Some droplets smaller than the initial size of CPC/Tween80 were also present. Thus the very large ΔZ_{ave} observed for CPC/Tween80 is attributable to both mucin binding to the NE droplets and mucin induced droplet aggregation. In contrast, DODAC/Tween80 did not aggregate into larger droplets or form smaller droplets upon interacting with mucin (Figure 5D). DODAC/Tween80 did indeed bind mucin, as evidenced by the homogenous layer of mucin coating the emulsion surface. Tween80 0:6 did not coalesce and had no associated mucin, as a homogenous field of mucin was observed, with no sequestration of mucin around the particle.

Thus, both NEs with large ΔZ_{ave} and large ΔZP values, and those with small ΔZ_{ave} and large ΔZP values are mucoadhesive but have different morphological properties upon binding mucin. In contrast, NEs with neither changes in ΔZ_{ave} nor ΔZP upon mucin addition do not appear to interact with mucin. The magnitude of ΔZP therefore is indicative of the degree of mucin binding, while ΔZ_{ave} describes both mucin association and particle structure upon binding. Both of these biophysical parameters are thus pertinent in evaluating NE mucoadhesion.

NE-Antigen Uptake in Nasal Epithelial Cells

To examine how the biophysical properties pertinent to NE-mucin association as observed by these *in vitro* assays translated to cellular systems, NE-OVA binding and uptake were studied in RPMI 2650 human nasal epithelial cells. RPMI 2650 cells express mucin1, the transmembrane isoform of mucin throughout the membrane, and have been used to study uptake through mucous barriers. [31-34] Cells were treated for 1.5 h at 4 °C or 37 °C with either 0.1% CAB/Tween80 1:6, Tween80 0:6, CPC/Tween80 1:40 or 1:6, DODAC/Tween80 1:6, or CPC/P407 1:6 containing 20 μg/mL of fluorescent A488-OVA. Treatment at 4 °C allowed examination of NE-OVA cell surface binding without active uptake, whereas at 37 °C both binding and uptake could be observed. CAB/Tween80 and Tween80 0:6 did not significantly enhance OVA retention on the cell surface at 4 °C or uptake at 37 °C (Figures 6I and 6II A & B) relative to A488-OVA treatment alone (not shown). CPC/Tween80 1:40 and 1:6 enhanced the levels of surface bound antigen at 4°C, suggesting increased adhesion of NE-OVA to membrane associated mucin (Figures 6I C & D). CPC/Tween80 1:6 enhanced adhesion more than 1:40, giving more intense areas of fluorescence on the cell surface, consistent with the trends observed through SPR and DLS/ZP measurements. Interestingly, DODAC/Tween80 and CPC/P407 also substantially enhanced OVA binding to the cell membrane at 4°C, but appeared to coat the membrane more uniformly in a greater number of cells than CPC/Tween80 1:6 which showed much more intense fluorescent puncta on the membrane in a fewer percentage of cells at this temperature (Figure 6I E & F). This may reflect the TEM observations of mucin induced aggregation of CPC/Tween80 1:6, as compared to DODAC/Tween80 and CPC/P407 which did not coalesce upon binding mucin. Increased surface adhesion led to enhanced intracellular uptake at 37 °C of NE-OVA for CPC/Tween80 1:40 and 1:6, with 1:6 inducing greater uptake than 1:40. DODAC/Tween80 and CPC/P407 also dramatically enhanced OVA uptake. DODAC/Tween80 induced significantly greater uptake than CPC/Tween80 1:6, however CPC/Tween80-OVA appeared to be localized in intense punctae of intracellular fluorescence in fewer cells than DODAC/Tween80-OVA, which had a more disperse distribution of OVA punctae within a greater number of cells (Figure 6II D & E). These results were confirmed by quantitation of the number of fluorescent cells using flow cytometry (Figure S6 and discussion). These intracellular punctae may correspond to NE-OVA localized in early endosomes or lysosomes. The distinct changes in the distribution pattern of antigen between 4°C and 37°C suggest that the majority of the antigen is associated with the cell surface and not internalized at 4°C, whereas the majority of the antigen is taken up intracellularly at 37°C.

To further confirm the intracellular localization of antigen at 37°C, the plasma membrane was stained with a fluorescent marker after NE-OVA treatment (Figure S7). We found that the majority, if not all of the A488-OVA fluorescence was localized within the confines of the plasma membrane, demonstrating that at 37°C, the majority of the antigen is not simply associated with the membrane, but is internalized. Furthermore, the 37°C treatment was repeated with DQ-OVA (Life Technologies, Carlsbad, CA), ovalbumin labeled with a self-quenched fluorescent dye, in place of A488-OVA (data not shown). The fluorescence of DQ-OVA remains quenched until ovalbumin is proteolytically processed, after which, fluorescence is emitted. A similar, though less intense pattern of intracellular fluorescence was observed for the NEs shown in figure 6II (intracellular fluorescent punctae for CPC/Tween80 1:40, 1:6, and DODAC/Tween80 and CPC/P407), confirming that the majority of the antigen was taken up intracellularly and proteolytically processed through antigen processing pathways for these NEs under these specific treatment conditions. Thus, prolonged NE-OVA adhesion to the cellular surface appears to facilitate increased intracellular antigen uptake.

Antigen Uptake in the Nasal Septa

The effect of NE composition on the uptake efficiency in the nasal epithelium was evaluated *in vivo*. To visualize antigen distribution, mice were immunized intranasally with 10 μg green fluorescent protein (GFP) alone or with 20% NE, and sacrificed 16-18 hr post-inoculation. Nasal septa were sectioned and imaged (Figure 7). Immunization with GFP alone resulted in diffuse background fluorescence (Figure 7A). Tween80 0:6-GFP showed similar diffuse fluorescence, likely attributable to nonspecific association of GFP or GFP-NE (Figure 7B). However, the fluorescence was slightly more localized than in mice receiving GFP alone, possibly reflecting concentration of multiple GFP molecules on the Tween80 0:6 droplets. The negative charge of SDS/Tween80 1:6 appeared to prevent nonspecific association with the mucosa, as no fluorescence was observed upon treatment (Figure 7C). In contrast, the positively charged CPC/Tween80 1:6 gave more intense fluorescence on the mucosa in punctate areas, reflecting antigen uptake into the nasal epithelium (Figure 7D). The anatomical structure of the nasal epithelium is depicted by Light Green Counterstaining and TUNEL staining of the nuclei of tissue sections from a mouse immunized with PBS only (Figure 7E). These results confirm that greater mucoadhesion facilitates increased antigen (and presumably NE) uptake across the mucosal layer and into the epithelium.

Intranasal Immunogenicity

Lastly, to determine the relationship between mucoadhesion and immune response induction, C57BL/6 mice were immunized IN with 20% NE of the CPC/Tween80 series (0:6, 1:40, 1:20, 1:6) containing 20 μg OVA, and boosted with the same formulation 4 weeks post-initial immunization (n=5 or 10 mice/formulation (see methods)). For the control group, mice were immunized with the same dose of OVA alone in PBS. Previous work by our group has demonstrated that intranasal immunization with CPC/Tween80 1:6 alone without antigen elicited no antigen specific IgG production. Thus, we chose not to include this control group in the present study. [35] We selected the CPC/Tween80 series to evaluate NEs with the same cationic and nonionic surfactants, and this series of emulsions showed a range of mucoadhesive properties. Serum anti-OVA specific IgG was measured at 2, 4, and 6-weeks post-initial immunization, and end-point titers were determined at 6 weeks (Figure 8A & B). Average anti-OVA IgG increased as the CPC was increased (Figure 8A). CPC/Tween80 1:6 treated mice had higher specific IgG levels than those immunized with lower CPC containing formulations even 2 and 4 weeks post-immunization. All NEs elicited higher responses than OVA alone except Tween80 0:6 which had IgG levels similar to antigen alone. Repeated immunization further magnified the differences between the emulsions (Figure 8A).

Vaccination with all formulations containing NE and OVA resulted in significantly higher IgG endpoint titers than vaccination with OVA alone (Figure 8B). End titrations of sera from individuals showed that at lower CPC, variation in the magnitude of the IgG response was greater than at high CPC. Mice in the 0:6 group had IgG titers ranging from very low (equivalent to OVA alone) to one having the same high titer as the 1:6 treated mice (1×10^5). Other mice in the 0:6 group had moderate responses with titers between 0.5-1×10^4. Increasing CPC to 1:40 gave similar variation, however a larger proportion of the group exhibited titers of 1×10^5. Further increasing CPC reduced the variation in IgG, and all mice in the 1:6 group had high end-titers between 0.5-1×10^5.

Thus, improving the mucoadhesion of the CPC/Tween80 NEs by increasing the CPC ratio increased both the magnitude and consistency of the immune response. Through ultracentrifugation separation, we determined that the majority of the OVA (>50-90%) is present on the NE droplet versus free in solution (supplementary info. and Figure S3). While the presence of increasing amounts of CPC does lead to slightly enhanced antigen incorporation, and may influence immunogenicity, immunization with other NE formulations which contained similar levels of antigen incorporation as CPC/Tween80 1:6 (such as CAB/Tween80 1:6 discussed below) elicited very different degrees of immunogenicity. Thus these trends in immunogencity for the CPC/Tween80 series are likely mostly attributable to the differences in mucoadhesion.

As some of the mice in each of the groups that were immunized with NE-OVA had the same endpoint total IgG titer as the mice in the CPC/Tween80 1:6 group (Figure 8B), IgG1 and

IgG2b subclass titers were measured to see whether there was a difference in the antibody response type. No significant differences were observed in the ratio between IgG2b and IgG1 for the mice which showed the same total IgG titer between groups (data not shown), suggesting that at this dosage and with OVA as the antigen, there was no difference in response type as CPC was increased.

To further corroborate the relationship between mucin association and immunogenicity, we looked at the effects of using zwitterionic CAB in lieu of CPC with Tween80. C57BL/6 mice were immunized IN as above with 20% CPC/Tween80 1:6 or CAB/Tween80 1:6 with 20 μg OVA. CAB/Tween80 elicited minimal serum IgG compared to CPC/Tween80 1:6 at all time points, even post-boost (Figure 8C). These results further suggest that mucoadhesion is necessary for intranasal adjuvanticity and can be used in selecting potential vaccine candidates.

DISCUSSION

Adjuvants enhance immune response induction through several mechanisms, including through a depot effect, which promotes prolonged stimulation of antibody producing cells. [15, 16] For IN vaccines the mucosa provides a site for sustained adhesion, and adjuvants with greater mucoadhesive capacity are likely to be more effective in immune response induction. In the present study, we demonstrate the effectiveness of NE based vaccines consisting of ionic and nonionic surfactants for IN immunization of the model antigen, ovalbumin in mice. Extensive *in vitro* biophysical characterization and cellular studies provided evidence supporting the hypothesis that NE-mucin association is critical for antigen uptake and induction of immunogenicity *in vivo*. These results are consistent with those observed for particulate based vaccines including chitosan and its derivatives with and without poly(lactic-co-glycolic acid) (PLGA) which increase the nasal residence time of antigens delivered IN and enhance antigen (or drug) permeation through the mucosa leading to improved efficacy. [36, 37]. NEs are composed of surfactants and oil with very different physicochemical properties than PLGA and chitosan, and provide different advantages over particulate systems for vaccine formulation. Here we demonstrate that *in vitro* mucin binding properties of nanoemulsion based vaccines directly relate to immunogenicity *in vivo*, and can provide valuable information on the potential efficacy of IN adjuvants.

NEs containing cationic surfactants had greater mucin affinity than uncharged or anionic emulsions, which showed little association with mucin. The critical role played by positive charge is consistent with observations made for other polymer-based micro- and nanoparticulates. [26, 38] However, our results also point to involvement of other parameters including surfactant hydrophobicity and polar head group structure in dictating the interaction of emulsions with mucin. This was illustrated by the CPC/Tween80 1:6 and DODAC/Tween80 1:6 NEs which have similar charges and surfactant ratios, but displayed dramatic differences in ΔZ_{ave}, ΔZP and particle morphology upon mucin addition in solution as well as differences in their association with the cell surface. These findings suggest that while ionic interactions are strong determinants of mucoadhesion, nonionic interactions between the NE components and mucin also significantly influence adhesion to the mucosal surface.

NEs could be classified into three general groups based on changes in size and charge with mucin. While it is unclear whether smaller or larger droplets are more effective adjuvants, the importance of adhesion for antigen delivery was confirmed both *in vitro* (in an epithelial cell line), and *in vivo* upon IN administration. NEs (containing OVA) that associated with mucin also enhanced the amount of cell surface bound OVA, which led to increased cellular antigen uptake compared to OVA alone or OVA with NEs which did not bind mucin. Furthermore, mice immunized with CPC/Tween80 1:6-GFP had greater GFP retention on the mucosa and internalized by cells in the epithelium relative to the neutral and anionic NEs, Tween80 0:6-GFP and SDS/Tween80 1:6-GFP, respectively. While it is yet to be determined how NE-antigen droplets are taken up intracellularly, we found that adhesion is necessary for uptake. Interestingly, NE did not enhance uptake in DCs or macrophages *in vitro* (not shown), emphasizing the importance of mucoadhesion-facilitated epithelial cell antigen uptake, and supporting our observations on the pivotal role of ciliated epithelial cells in the NE-mediated immune response. [18]

NE-mucin interactions directly correlated with induction of a specific humoral immune response in mice immunized IN with the CPC/Tween80 series NEs containing OVA. Improving mucoadhesion by increasing the CPC content increased the average serum anti-OVA IgG, and reduced the intra-group variation in IgG titers. In contrast, the zwitterionic CAB/Tween80, which did not bind mucin, did not induce an IgG response. Greater retention of NE-antigen likely allows prolonged stimulation of immune responders by slowing vaccine removal through mucociliary clearance. CPC/Tween80 1:6 provides the most sustained OVA release at the application site, thus facilitating uptake leading to the induction of a more consistent IgG response via a stronger depot effect. Furthermore, enhanced epithelial cell uptake promotes intracellular antigen retention which perhaps also enhances transfer to DCs through phagocytosis. [39] While OVA-specific mucosal IgA levels in bronchial-alveolar-lavages was insignificant (not shown), we previously observed that NE induced IgA in bronchial-alveolar-lavages for other more immunogenic antigens such as anthrax protective antigen [21]. Our results are consistent with studies demonstrating that improving mucin association of polymer-based micro- and nanoparticulate such as PLGA by coating them with cationic moieties such as N-trimethyl chitosan (TMC) enhanced systemic and mucosal antigen specific antibody production. [26, 38, 40]. Thus, lack of NE-mucin association as assessed by these relatively simple biophysical assays based on DLS, ZP and SPR *in vitro* is an effective indicator of a poor intranasal adjuvant. While increasing the cationic charge can lead to improved mucoadhesion and immunogenicity, we have observed that excessive positive charge leads to greater cellular toxicity. Therefore, using these assays to better understand the nonionic interactions between emulsion components and mucin will allow for further formulation optimization. Although it remains to be explored how the changes in particle integrity upon interacting with mucus influence immunogencity, these assays provide valuable information for prescreening lead formulations, and give insight into how they will interact with the mucosa *in vivo*.

Activation of a protective immune response is clearly a multifactorial process, with the physical delivery of antigen and adjuvant being just one parameter dictating vaccine effectiveness. We have previously shown that NEs serve as much more than inert vehicles for antigen delivery, and that these formulations are able to activate cytokine production by epithelial cells in the nasal passage, and induce DC trafficking. [18] The simple *in vitro* screening methods presented here along with our *in vivo* immunogencity studies provide the first steps to understanding the relationship between the physicochemical properties of emulsion surfactants and adjuvant effectiveness. We demonstrate that NEs with very diverse sets of surface and adhesion properties can be produced by variation of the surfactant combinations. These differences likely impact non-adhesion related activities as well, and we are expanding our *in vivo* immunogenicity studies to NEs with other surfactant compositions in the library to better understand these relationships. Other parameters influencing vaccine effectiveness are also currently being pursued in our laboratory including the effects of NE on cellular immune response activation, antigen permeability enhancement (opening of tight junctions), antigen release kinetics, and upregulation of immunostimulatory genes. While mucoadhesion constitutes only the initial step of NE delivery and uptake leading to induction of immunogenicity, without the ability to adhere to the mucosa, NE adjuvanticity is severely compromised. Thus these simple *in vitro* screening methods with high throughput capacity provide a valuable tool for mucosal vaccine candidate selection, and for the design and optimization of more effective mucosal adjuvants.

Supplementary Material

Refer to Web version on PubMed Central for supplementary material.

Acknowledgments

This project has been funded in whole or in part with Federal funds from the National Institute for Allergy and Infectious Disease, National Institutes of Health, Department of Health and Human Services, under Contract No.HHSN272200900031C. Dr. James R. Baker Jr. holds an ownership stake in NanoBio, Corp., and is the inventor of technologies that the University has licensed to NanoBio, Corp. Some of these technologies are involved in this research, and NanoBio, Corp. is a subcontractor in this research to create the nanoemulsion formulations. NanoBio, Corp. has no role in the study design of the work performed at UM, the data collection and analysis, the decision to publish, or the preparation of the manuscript unless such manuscript is clearly collaborative. All confocal and electron microscopy were performed on equipment at the University of Michigan Microscopy and Imaging Analysis Laboratory (MIL). We thank Dr. Stephen Gracon at NanoBio, Corp. for helpful discussions, Dr. Jakub Simon at NanoBio, Corp. for statistical analysis and helpful discussions, and Dr. Seok Ki Choi at the University of Michigan for SPR data analysis assistance and critical review of the manuscript.

ABBREVIATIONS

NE	nanoemulsion
DLS	dynamic light scattering
ZP	zeta potential
IN	intranasal
HBsAg	Hepatitis B surface antigen
PS	particle size
ZP_{init}	initial Z prior to mucin addition

ZP_{final}	final ZP after mucin addition
ΔZ_{ave}	change in particle size with mucin
ΔZP	change in ZP with mucin
HLB	hydrophilic-lipophilic balance
SPR	surface plasmon resonance
TEM	transmission electron microscopy
GFP	green fluorescent protein
OVA	ovalbumin

REFERENCES

1. Davis SS. Nasal vaccines. Adv Drug Deliv Rev. 2001; 51(1-3):21–42. [PubMed: 11516777]
2. Freytag LC, Clements JD. Mucosal adjuvants. Vaccine. 2005; 23(15):1804–13. [PubMed: 15734046]
3. Holmgren J, Czerkinsky C. Mucosal immunity and vaccines. Nat Med. 2005; 11(4 Suppl):S45–53. [PubMed: 15812489]
4. Vajdy M, Singh M. The role of adjuvants in the development of mucosal vaccines. Expert Opin Biol Ther. 2005; 5(7):953–65. [PubMed: 16018740]
5. Neutra MR, Kozlowski PA. Mucosal vaccines: the promise and the challenge. Nat Rev Immunol. 2006; 6(2):148–58. [PubMed: 16491139]
6. Mestecky J, Moldoveanu Z, Russell MW. Immunologic uniqueness of the genital tract: challenge for vaccine development. Am J Reprod Immunol. 2005; 53(5):208–14. [PubMed: 15833098]
7. Wizel B, Persson J, Thorn K, Nagy E, Harandi AM. Nasal and skin delivery of IC31((R))-adjuvanted recombinant HSV-2 gD protein confers protection against genital herpes. Vaccine. 2012; 30(29):4361–8. [PubMed: 22682292]
8. Costantino HR, Illum L, Brandt G, Johnson PH, Quay SC. Intranasal delivery: physicochemical and therapeutic aspects. Int J Pharm. 2007; 337(1-2):1–24. [PubMed: 17475423]
9. Kemble G, Greenberg H. Novel generations of influenza vaccines. Vaccine. 2003; 21(16):1789–95. [PubMed: 12686096]
10. Van Kampen KR, Shi Z, Gao P, Zhang J, Foster KW, Chen DT, Marks D, Elmets CA, Tang DC. Safety and immunogenicity of adenovirus-vectored nasal and epicutaneous influenza vaccines in humans. Vaccine. 2005; 23(8):1029–36. [PubMed: 15620476]
11. Treanor JJ, Mattison HR, Dumyati G, Yinnon A, Erb S, O'Brien D, Dolin R, Betts RF. Protective efficacy of combined live intranasal and inactivated influenza A virus vaccines in the elderly. Ann Intern Med. 1992; 117(8):625–33. [PubMed: 1530193]
12. Treanor J, Wu H, Liang H, Topham DJ. Immune responses to vaccinia and influenza elicited during primary versus recent or distant secondary smallpox vaccination of adults. Vaccine. 2006; 24(47-48):6913–23. [PubMed: 17014939]
13. Obrosova-Serova NP, Slepushkin AN, Kendal AP, Harmon MW, Burtseva EI, Bebesheva NI, Beljaev AL, Lonskaja NI, Medvedeva TE, Egorov AY, et al. Evaluation in children of cold-adapted influenza B live attenuated intranasal vaccine prepared by reassortment between wild-type B/Ann Arbor/1/86 and cold-adapted B/Leningrad/14/55 viruses. Vaccine. 1990; 8(1):57–60. [PubMed: 2180233]
14. Haneberg B, Dalseg R, Wedege E, Hoiby EA, Haugen IL, Oftung F, Andersen SR, Naess LM, Aase A, Michaelsen TE, Holst J. Intranasal administration of a meningococcal outer membrane vesicle vaccine induces persistent local mucosal antibodies and serum antibodies with strong bactericidal activity in humans. Infect Immun. 1998; 66(4):1334–41. [PubMed: 9529050]

15. Zinkernagel RM, Ehl S, Aichele P, Oehen S, Kundig T, Hengartner H. Antigen localisation regulates immune responses in a dose- and time-dependent fashion: A geographical view of immune reactivity. Immunol Rev. 1997; 156:199–209. [PubMed: 9176709]
16. Storni T, Kundig TM, Senti G, Johansen P. Immunity in response to particulate antigen-delivery systems. Adv Drug Deliver Rev. 2005; 57(3):333–355.
17. Makidon PE, Bielinska AU, Nigavekar SS, Janczak KW, Knowlton J, Scott AJ, Mank N, Cao ZY, Rathinavelu S, Beer MR, Wilkinson JE, Blanco LP, Landers JJ, Baker JR. Pre-Clinical Evaluation of a Novel Nanoemulsion-Based Hepatitis B Mucosal Vaccine. Plos One. 2008; 3(8)
18. Makidon PE, Belyakov IM, Blanco LP, Janczak KW, Landers J, Bielinska AU, Groom JV 2nd, Baker JR Jr. Nanoemulsion mucosal adjuvant uniquely activates cytokine production by nasal ciliated epithelium and induces dendritic cell trafficking. Eur J Immunol. 2012
19. Stanberry LR, Simon JK, Johnson C, Robinson PL, Morry J, Flack MR, Gracon S, Myc A, Hamouda T, Baker JR. Safety and immunogenicity of a novel nanoemulsion mucosal adjuvant W(80)5EC combined with approved seasonal influenza antigens. Vaccine. 2012; 30(2):307–316. [PubMed: 22079079]
20. Bielinska AU, Chepurnov AA, Landers JJ, Janczak KW, Chepurnova TS, Luker GD, Baker JR. A novel, killed-virus nasal vaccinia virus vaccine. Clin Vaccine Immunol. 2008; 15(2):348–358. [PubMed: 18057181]
21. Bielinska AU, Janczak KW, Landers JJ, Makidon P, Sower LE, Peterson JW, Baker JR J. r. Mucosal immunization with a novel nanoemulsion-based recombinant anthrax protective antigen vaccine protects against Bacillus anthracis spore challenge. Infection and Immunity. 2007; 75(8): 4020–4029. [PubMed: 17502384]
22. Bielinska AU, Janczak KW, Landers JJ, Markovitz DM, Montefiori DC, Baker JR. Nasal immunization with a recombinant HIV gp120 and nanoemulsion adjuvant produces th1 polarized responses and neutralizing antibodies to primary HIV type 1 isolates. Aids Res Hum Retrov. 2008; 24(2):271–281.
23. Baos SC, Phillips DB, Wildling L, McMaster TJ, Berry M. Distribution of sialic acids on mucins and gels: a defense mechanism. Biophys J. 2012; 102(1):176–84. [PubMed: 22225812]
24. Lai SK, Wang YY, Hanes J. Mucus-penetrating nanoparticles for drug and gene delivery to mucosal tissues. Adv Drug Deliv Rev. 2009; 61(2):158–71. [PubMed: 19133304]
25. Bansil R, Stanley E, LaMont JT. Mucin biophysics. Annu Rev Physiol. 1995; 57:635–57. [PubMed: 7778881]
26. Pawar D, Goyal AK, Mangal S, Mishra N, Vaidya B, Tiwari S, Jain AK, Vyas SP. Evaluation of mucoadhesive PLGA microparticles for nasal immunization. AAPS J. 2010; 12(2):130–7. [PubMed: 20077052]
27. Takeuchi H, Thongborisute J, Matsui Y, Sugihara H, Yamamoto H, Kawashima Y. Novel mucoadhesion tests for polymers and polymer-coated particles to design optimal mucoadhesive drug delivery systems. Adv Drug Deliv Rev. 2005; 57(11):1583–94. [PubMed: 16169120]
28. Thongborisute J, Takeuchi H. Evaluation of mucoadhesiveness of polymers by BIACORE method and mucin-particle method. Int J Pharm. 2008; 354(1-2):204–9. [PubMed: 18207675]
29. He P, Davis SS, Illum L. In vitro evaluation of the mucoadhesive properties of chitosan microspheres. International Journal of Pharmaceutics. 1998; 166(1):75–88.
30. Choi SK, Myc A, Silpe JE, Sumit M, Wong PT, McCarthy K, Desai AM, Thomas TP, Kotlyar A, Holl MM, Orr BG, Baker JR Jr. Dendrimer-based multivalent vancomycin nanoplatform for targeting the drug-resistant bacterial surface. ACS Nano. 2013; 7(1):214–28. [PubMed: 23259666]
31. Wengst A, Reichl S. RPMI 2650 epithelial model and three-dimensional reconstructed human nasal mucosa as in vitro models for nasal permeation studies. Eur J Pharm Biopharm. 2010; 74(2): 290–7. [PubMed: 19733661]
32. Bai S, Yang T, Abbruscato TJ, Ahsan F. Evaluation of human nasal RPMI 2650 cells grown at an air-liquid interface as a model for nasal drug transport studies. J Pharm Sci. 2008; 97(3):1165–78. [PubMed: 17628494]
33. Kissel T, Werner U. Nasal delivery of peptides: an in vitro cell culture model for the investigation of transport and metabolism in human nasal epithelium. J Control Release. 1998; 53(1-3):195–203. [PubMed: 9741927]

34. Harikarnpakdee S, Lipipun V, Sutanthavibul N, Ritthidej GC. Spray-dried mucoadhesive microspheres: preparation and transport through nasal cell monolayer. AAPS PharmSciTech. 2006; 7(1):E12. [PubMed: 16584142]

35. Bielinska AU, Gerber M, Blanco LP, Makidon PE, Janczak KW, Beer M, Swanson B, Baker JR Jr. Induction of Th17 cellular immunity with a novel nanoemulsion adjuvant. Crit Rev Immunol. 2010; 30(2):189–99. [PubMed: 20370629]

36. Mangal S, Pawar D, Garg NK, Jain AK, Vyas SP, Rao DS, Jaganathan KS. Pharmaceutical and immunological evaluation of mucoadhesive nanoparticles based delivery system(s) administered intranasally. Vaccine. 2011; 29(31):4953–62. [PubMed: 21575664]

37. Kang ML, Cho CS, Yoo HS. Application of chitosan microspheres for nasal delivery of vaccines. Biotechnol Adv. 2009; 27(6):857–65. [PubMed: 19583998]

38. Slutter B, Bal S, Keijzer C, Mallants R, Hagenaars N, Que I, Kaijzel E, van Eden W, Augustijns P, Lowik C, Bouwstra J, Broere F, Jiskoot W. Nasal vaccination with N-trimethyl chitosan and PLGA based nanoparticles: nanoparticle characteristics determine quality and strength of the antibody response in mice against the encapsulated antigen. Vaccine. 2010; 28(38):6282–91. [PubMed: 20638455]

39. Myc A, Kukowska-Latallo JF, Smith DM, Passmore C, Pham T, Wong P, Bielinska AU, Baker JR Jr. Nanoemulsion nasal adjuvant W(8)(0)5EC induces dendritic cell engulfment of antigen-primed epithelial cells. Vaccine. 2013; 31(7):1072–9. [PubMed: 23273511]

40. Tafaghodi M, Saluja V, Kersten GF, Kraan H, Slutter B, Amorij JP, Jiskoot W. Hepatitis B surface antigen nanoparticles coated with chitosan and trimethyl chitosan: Impact of formulation on physicochemical and immunological characteristics. Vaccine. 2012; 30(36):5341–8. [PubMed: 22749834]

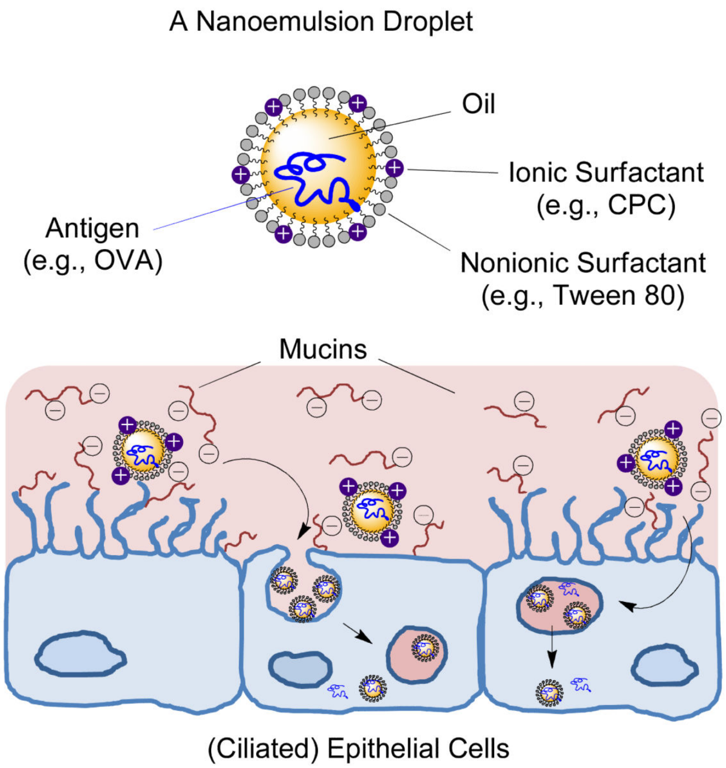

Figure 1.

Structure of a nanoemulsion (NE) droplet and illustration of NE-mediated antigen delivery through the nasal epithelial layer as facilitated by NE-mucin interactions. (cetylpyridinium chloride (CPC), ovalbumin (OVA))

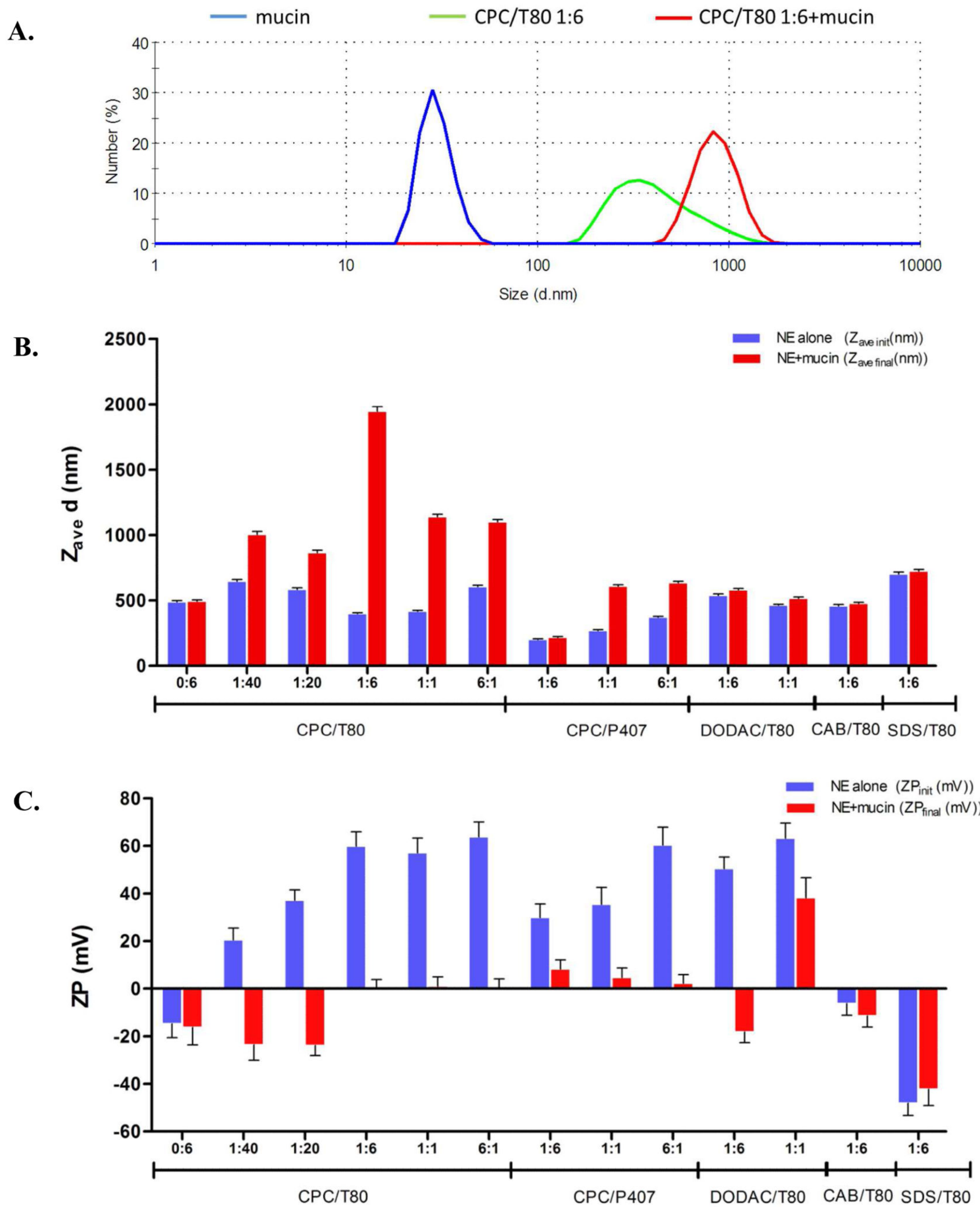

Figure 2.

(A) Number weighted size distribution of 0.05 mg/mL mucin alone (blue), 0.1% NE (CPC/Tween80 1:6) alone (green), or the co-incubated mixture at the same final concentrations (red). (B) Representative NE Z_{ave} values prior to ($Z_{ave\ init}$) and after ($Z_{ave\ final}$) mucin addition. (C) ZP values prior to (ZP_{init}) and after (ZP_{final}) mucin addition. Error bars for Z_{ave} measurements represent standard deviation as calculated from PdI values, or zeta deviation for ZP measurements. (ΔZave and ΔZP values are plotted in Figure S2)

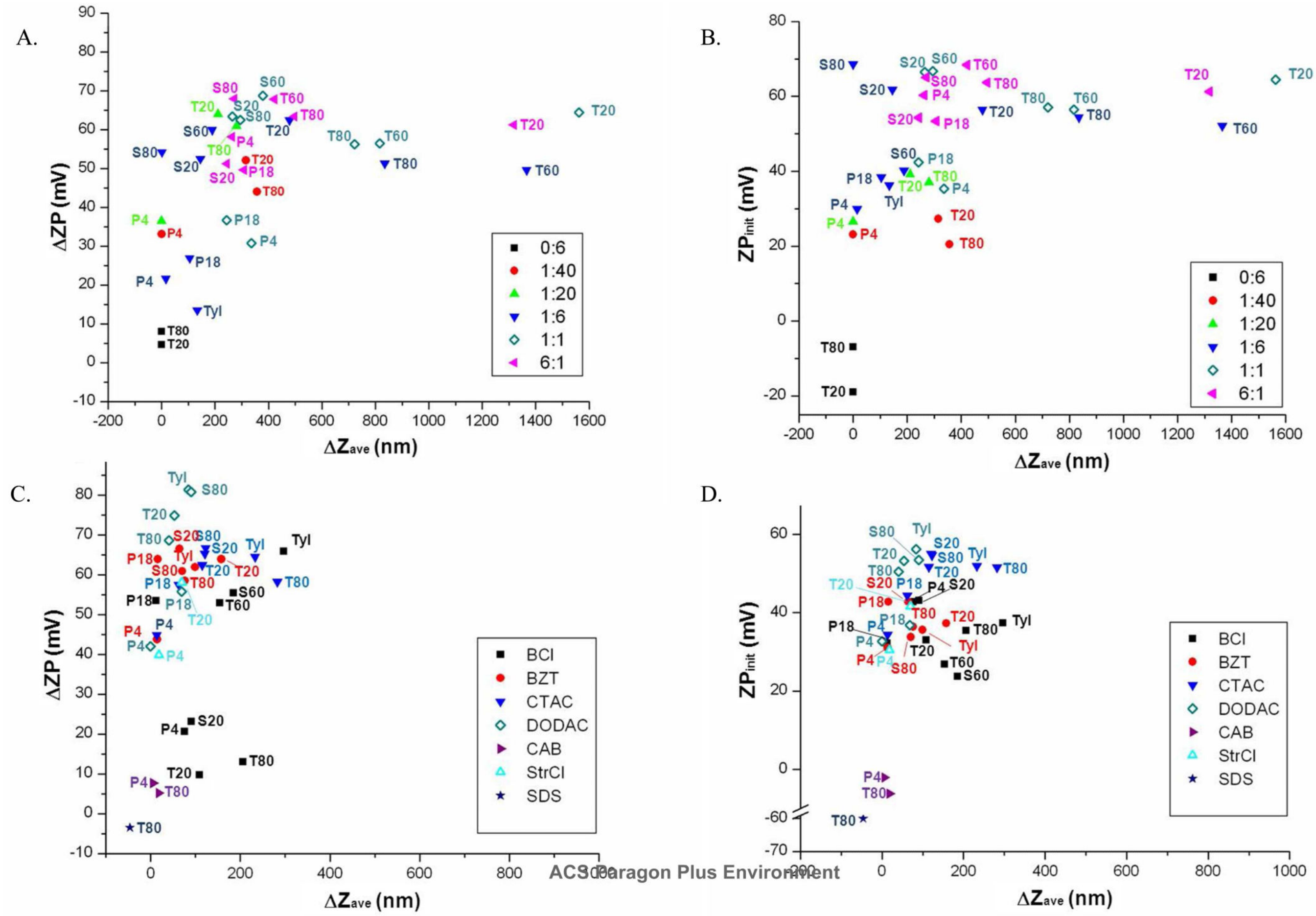

Figure 3.

Scatter plots of ΔZP vs. ΔZ_{ave} upon mucin addition (0.05 mg/mL) for NE formulations (0.1%) containing CPC at various surfactant ratios (A) or a non-CPC cationic surfactant at a 1:6 cationic:nonionic ratio (C). ZP_{init} vs. ΔZ_{ave} for the same CPC (B) or non-CPC (D) NEs with mucin. Surfactant abbreviations are as listed in Table 1.

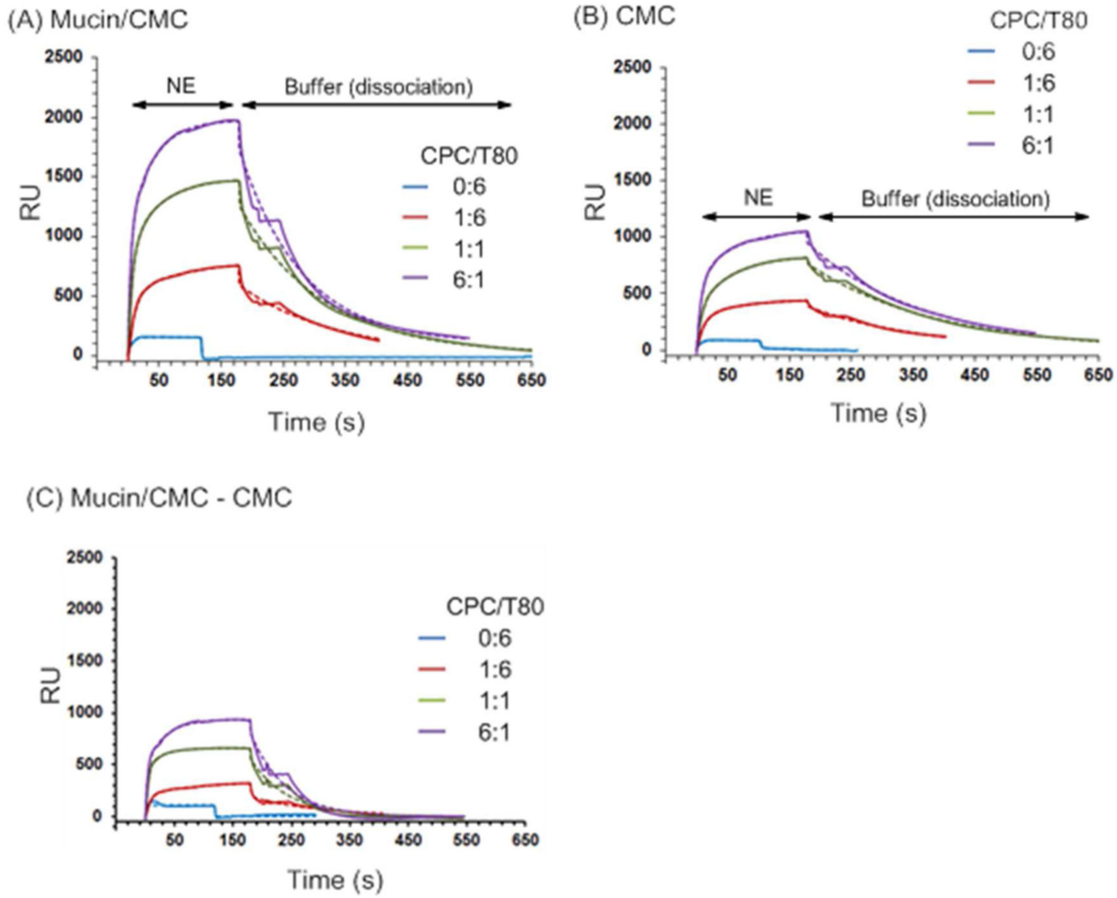

Figure 4.

SPR sensorgrams for the binding of NEs to (A) a mucin-immobilized carboxymethyl cellulose (Mucin/CMC) dextran surface (flow cell 1 (Fc1)), and (B) a CMC dextran only reference surface (flow cell 2 (Fc2)). 0.0125% of the CPC/Tween80 series (0:6, 1:6, 1:1, or 6:1) NEs were injected on the surface in 1 mM HEPES, pH 7. (C) Subtracted sensorgrams where $\Delta RU = RU_{Fc1} - RU_{Fc2}$. Sensorgrams are shown as solid lines and curve fits as dashed lines.

NIH-PA Author Manuscript

NIH-PA Author Manuscript

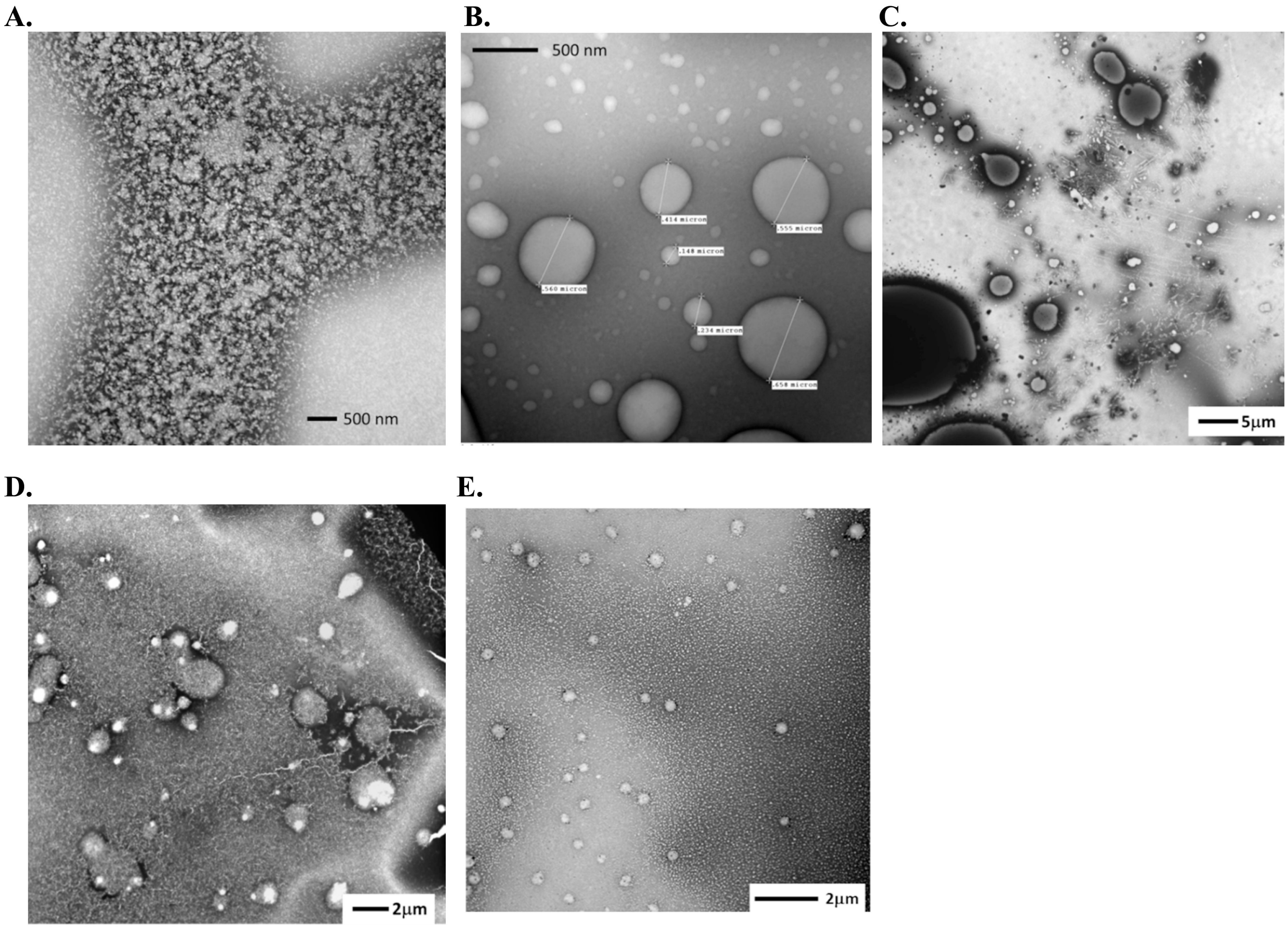

Figure 5.
TEM of mucin alone (A), CPC/Tween80 1:6 alone (B), and mucin with CPC/Tween80 1:6 (C), DODAC/Tween80 1:6 (D), or Tween80 0:6 (E) in 1 mM HEPES pH 7.

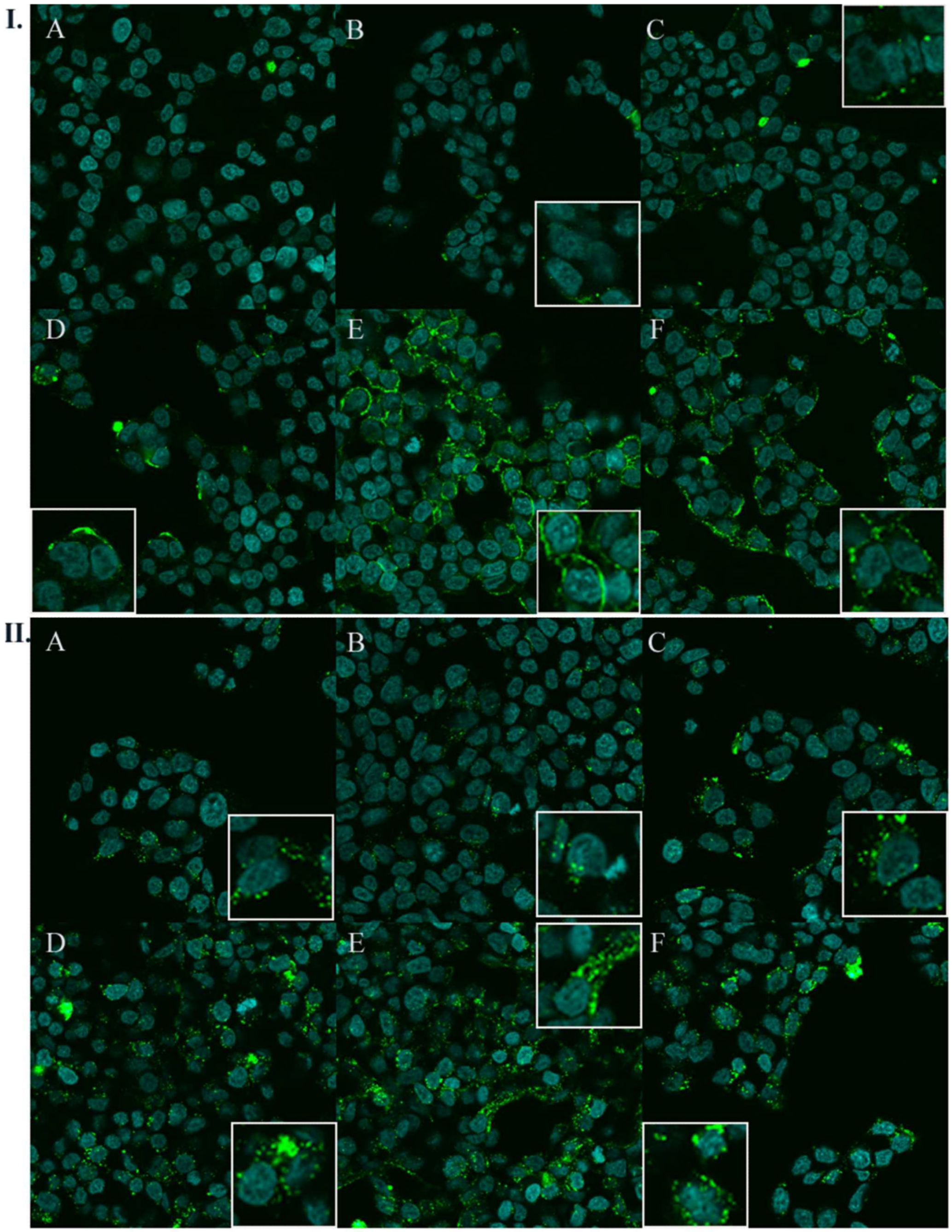

Figure 6.

Confocal fluorescence microscopy of RPMI 2650 cells treated 1.5 h at (I) 4 °C or (II) 37 °C with 20 μg/mL A488-OVA (green fluorescence) with (A) 0.1% CAB/Tween80 1:6, (B) Tween80 0:6, (C) CPC/Tween80 1:40, (D) CPC/Tween80 1:6, (E) DODAC/Tween80 1:6, or (F) CPC/P407 1:6. Nuclei were stained with DAPI (blue fluorescence).

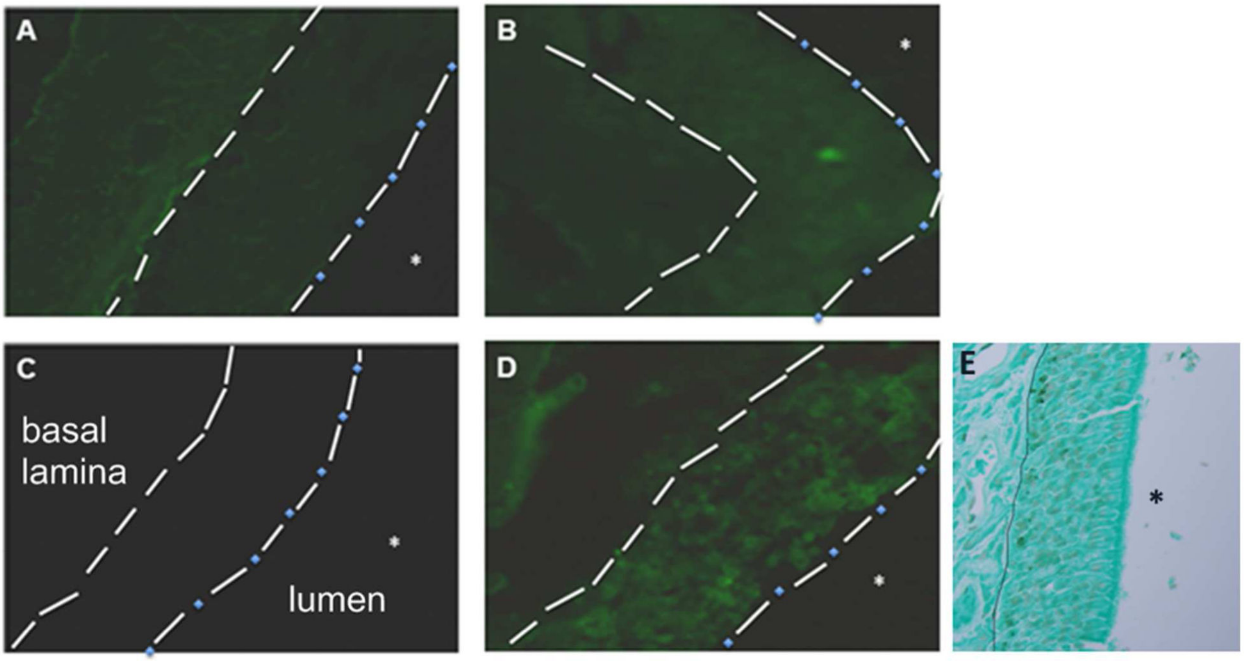

Figure 7.

Fluorescence images (400×) of frozen sectioned nasal septal tissue isolated from mice immunized with (A) GFP alone, or GFP with (B) Tween80 0:6, (C) SDS/Tween80 1:6, or (D) CPC/Tween80 1:6. Features indicated: septal columnar epithelium (between dashed lines), basal lamina (dashed line), epithelial-luminal junction (dash-dotted line), and nasal lumen (*). (E) Light micrograph of a Light Green Counterstain and TUNEL stained paraffin section of the nasal epithelium from a mouse immunized with PBS alone is provided as an anatomical reference. The solid line represents the basal lamina, and the nasal lumen is indicated (*).

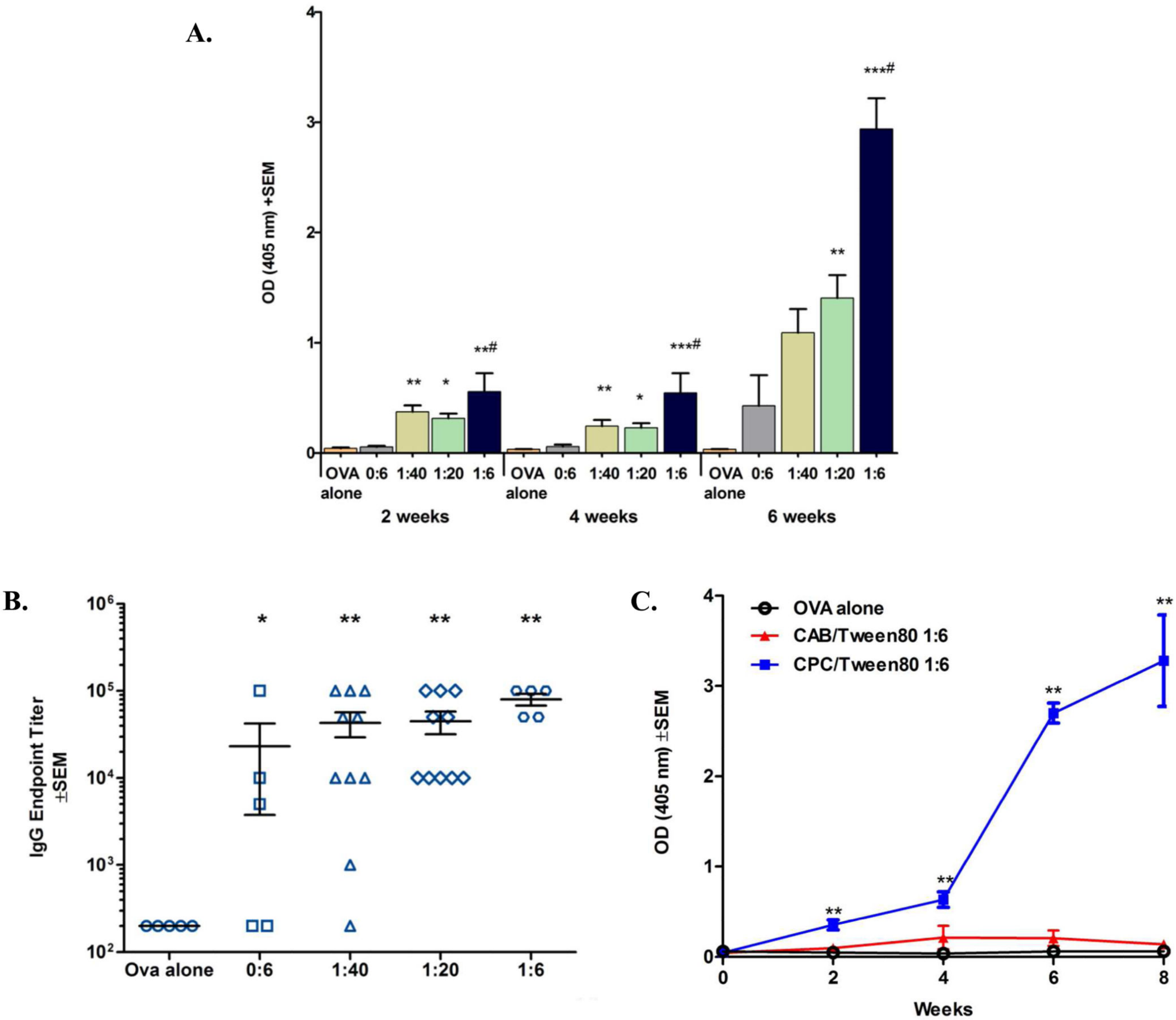

Figure 8.

Serum anti-OVA IgG after IN immunization with 20 μg OVA alone or with 20% CPC/Tween80 NEs (0:6, 1:40, 1:20, 1:6) (A) Average anti-OVA IgG at 2, 4, and 6-weeks post initial immunization for 1:200 serum dilution. *p<0.05; **p<0.01; ***p<0.001 versus OVA alone; and $^{\#}$p<0.05 versus 0:6 with OVA using Kruskal-Wallis with Dunn's adjustment for multiple comparisons. (B) Serum anti-OVA IgG endpoint titers of individual mice 6-weeks post initial immunization. (C) Serum anti-OVA IgG from mice immunized IN with 20% CPC/Tween80 1:6 or CAB/Tween80 1:6 with 20 μg OVA as measured by ELISA expressed as OD_{405nm} for serum diluted 1:200. *p<0.05; **p<0.01 versus OVA alone using Kruskal-Wallis with Dunn's adjustment for multiple comparisons.

NIH-PA Author Manuscript
NIH-PA Author Manuscript

Table 1

NE surfactants and abbreviations. Net charges of ionic surfactants at pH 7 are indicated.

Ionic Surfactants	Nonionic Surfactants
Cetylpyridinium Chloride (CPC) (+) Benzalkonium Chloride (BCI) (+) Stearalkonium chloride (StrCI) (+) Cetrimonium chloride (CTAC) (+) Benzethonium chloride (BZT) (+) Dioctadecyl dimethyl ammonium (DODAC) (+) Cocamidopropyl betaine (CAB) (zwitterion) Sodium dodecyl sulfate (SDS) (−)	Tween Series: Tween20 (T20), Tween60 (T60), Tween80 (T80) Span Series: Span20 (S20), Span60 (S60), Span80 (S80) Poloxamers: Poloxamerl88 (P18), Poloxamer407 (P4) Tvloxaool (Tvl)